PHYSICAL REVIEW D **86,** 095027 (2012)

Magic messengers in gauge mediation and signal for 125 GeV boosted Higgs boson

Pritibhajan Byakti*
Theory Division, Saha Institute of Nuclear Physics, 1/AF Bidhan Nagar, Kolkata 700064, India

Diptimoy Ghosh†
Tata Institute of Fundamental Research, Homi Bhabha Road, Mumbai 400005, India
(Received 15 July 2012; published 26 November 2012)

We consider a renormalizable messenger sector with magic messenger fields instead of the usual SU(5) complete multiplets. We derive the soft supersymmetry breaking terms and show that the gaugino sector can be parametrized by only two parameters. These parameters can be chosen appropriately to obtain various patterns of gaugino masses and different ratios among them. The sfermion sector can also be characterized by two independent parameters which can be adjusted to change the relative masses of squarks and sleptons. A judicious choice of parameters also allows us to achieve the lightest Higgs boson mass, about 125 GeV. In this paper we focus on a scenario where a comparatively large hierarchy exists between the U(1) and SU(2) gaugino mass parameters. In such a case, the lightest Higgs boson originating from the decay of the next-to-lightest neutralino, following the direct production of a chargino neutralino pair, can be considerably boosted. We show that a boosted supersymmetric Higgs signal with a decent signal-to-background ratio can be obtained using the jet substructure technique at the LHC with 8 TeV (14 TeV) center-of-mass energy and an integrated luminosity of about 30 fb^{-1} (15 fb^{-1}).

DOI: 10.1103/PhysRevD.86.095027 PACS numbers: 14.80.Da, 12.60.−i, 12.60.Jv

I. INTRODUCTION

The performance of the Large Hadron Collider (LHC) at CERN has been extraordinary in the last year, and data of about 5 fb^{-1} have been already collected by each of the two major experimental groups, CMS and ATLAS. With the data already accumulated, the LHC has left the LEP and Tevatron results far behind in many of the search channels. But, apart from the recent hint [1,2] about a possible 124–126 GeV Higgs boson, no other signal of any new physics (NP) has been reported yet.

The minimally supersymmetric Standard Model (MSSM), which is undoubtedly one of the most studied models beyond the Standard Model (SM), has been a benchmark for the LHC searches, and limits on supersymmetric particles have been shown by both the ATLAS and CMS Collaborations [3].

Supersymmetry (SUSY) [4,5], which is a beautiful theoretical idea in its own right, has been in the spotlight among the phenomenologists for a long time because of its ability to elegantly tame the quadratic divergence in the scalar sector of the SM. However, if SUSY has to be realized in nature, it must be broken so that it does not contradict experimental observations. From a theoretical point of view, one would expect that the SUSY is broken spontaneously so that the underlying microscopic Lagrangian is SUSY invariant, but the vacuum state is not. This is the same mechanism that keeps the electroweak symmetry hidden at low energies. There is no consensus about how SUSY must be broken at high energies, but regardless of the way it is broken, at the electroweak scale the effect of SUSY breaking can always be parametrized by introducing additional terms in the Lagrangian that break SUSY explicitly. But these terms should only include operators that do not bring back the quadratic divergences from the quantum corrections to the scalar masses. These are called the SUSY breaking soft terms, all of which have positive mass dimension.

Unfortunately, spontaneous breaking of SUSY in a phenomenologically acceptable way with only tree-level renormalizable interactions has not been achieved until now. This problem has been solved by breaking SUSY in a sector, the so-called ''hidden sector,'' which has either no coupling or very small direct coupling to the MSSM fields. However, there are some mediating interactions that carry the information of SUSY breaking from the hidden sector to the MSSM and generate the soft terms. The gravitational interaction as a mediator of SUSY breaking has been the most popular scenario historically [6]. Another very popular mechanism has been the so-called ''gauge-mediated SUSY breaking (GMSB)'' [7–12] scenario, where the soft terms are generated through loops involving some messenger fields. These messenger fields couple to the SUSY breaking sector and also have SM gauge group quantum numbers. As gauge interactions are flavor diagonal, this mechanism also has the advantage of automatically being flavor blind, which is phenomenologically attractive from the points of view of flavor changing neutral currents.

The general gauge mediation (GGM), a framework developed by Meade, Seiberg, and Shih [13], generalizes

*pritibhajan.byakti@saha.ac.in
†diptimoyghosh@theory.tifr.res.in

models of gauge mediation to accommodate arbitrary hidden sectors, including those which are not necessarily weakly coupled. It was shown in GGM that the soft masses of MSSM gauginos and sfermions, to leading order in the SM gauge interactions, can be expressed in terms of the hidden sector current correlation functions. Extension of this framework has been studied in [14–20]. It was also shown in a model-independent way that nonuniversal gaugino masses can be obtained in GGM without spoiling the gauge-coupling unification. By universality in gaugino masses, we mean that these masses at any scale are proportional to the corresponding gauge couplings at that scale. However, in weakly coupled GMSB scenarios with complete multiplets of SU(5) messengers, the gaugino masses remain universal. In general messenger models [21,22], one can achieve nonuniversal gaugino masses, but the masses of the messenger fields get constrained in order to maintain gauge coupling unification.

It was shown in [23] that one can achieve unification of gauge couplings even if the new fields added at some intermediate scales do not form complete multiplets of SU(5) and the unification is independent of the scale at which these fields are added. These specially chosen fields were termed "magic" fields, and they were used in ordinary gauge mediation in order to get nonuniversal gaugino masses with extremely large hierarchy, 1:30:200, among the U(1), SU(2). and SU(3) gaugino mass parameters [23], which is phenomenologically not interesting. Also the obtained patterns of mass ratios were not very flexible.

In this paper we generalize their idea and write the superpotential containing all possible renormalizable terms for the messenger sector. We derive the soft SUSY breaking terms and show that the gaugino sector can be described by two independent parameters, which can be tuned to achieve almost any ratio of gaugino masses. This is a novel feature of our models. We also show that the sfermion sector in this class of models can also be parametrized by two parameters which can be chosen to adjust the relative masses of squarks and sfermions. In this class of models, the squark masses can be equal to the Higgs mass parameters m_{H_u} and m_{H_d} at the messenger scale, which can lead to a small value of the Higgsino mass parameter μ and thus a Higgsino-like next-to-lightest supersymmetric particle (NLSP) (like models of extra ordinary gauge mediation (EOGM) with doublet-triplet splitting [24]). Some regions of the parameter space of this model also allow for the lightest SUSY Higgs mass, about 125 GeV.

We consider a phenomenologically interesting scenario, where the ratio of the U(1) and SU(2) gaugino mass parameters at the electroweak scale is comparatively larger than the universal case 1:2. In this case, because of the comparatively larger splitting between the next-to-lightest neutralino lightest (χ_2^0) and the neutralino (χ_1^0), the Higgs boson (h) coming from the decay $\chi_2^0 \to \chi_1^0\ h$ is quite boosted. Motivated by this, we study the $\ell + b\bar{b} + \not{p}_T$ channel to look for a SUSY Higgs boson using the jet substructure technique.

The paper is organized as follows. In the next section we briefly review the concept of magic fields. In Sec. III, we describe our models and then study the mass spectrum of gauginos and sfermions. The phenomenology of an explicit model of this class of models is discussed in Sec. . We close our discussion in Sec. V with a brief summary of our findings.

II. MAGIC FIELDS AND UNIFICATION

In this section we will review the concept of magic fields and derive some relations that will be useful later in this paper. It is well known that, if no additional matter field is added in the intermediate scale, the SM gauge couplings get unified in the MSSM at the scale $M_0 \sim 2.0 \times 10^{16}$ GeV. In general, assuming that the gauge couplings unify at some scale $M_{\rm GUT}$, their one-loop renormalization group (RG) equations reads,

$$\alpha_a^{-1}(\mu) = -\frac{b^a}{2\pi}\ln\frac{\mu}{M_{\rm GUT}} + \alpha^{-1}(M_{\rm GUT}), \tag{1}$$

where the index $a = 1, 2, 3$ represents the SM gauge groups U(1), SU(2), and SU(3), respectively, and b_a are the corresponding beta functions. In the MSSM we have $b^a = b_0^a = \{\frac{33}{5}, 1, -3\}$.

At any value of μ, Eq. (1) is an equation of a straight line in α^{-1} and b. It directly follows that for the unification of the gauge couplings, α_a^{-1} and b_a must respect the following relation,

$$\frac{\alpha_3^{-1} - \alpha_2^{-1}}{\alpha_2^{-1} - \alpha_1^{-1}} = \frac{b^3 - b^2}{b^2 - b^1}. \tag{2}$$

Even if matter fields are added at some intermediate scale, the gauge coupling unification can be maintained (at one loop) so far as Eq. (2) is satisfied. The fields whose beta functions are such that they do not spoil Eq. (2) are called magic fields.

Using the one-loop RG equation of Eq. (1) in the MSSM one has,

$$\alpha_a^{-1}(M_Z) - \alpha_b^{-1}(M_Z) = -\frac{b_0^a - b_0^b}{2\pi}\log\frac{M_Z}{M_0}. \tag{3}$$

We now add matter fields at some intermediate scales and assume that fields added at the scale m_i contribute to the beta functions by an amount d_i^a (Dynkin index of that field). The gauge couplings at any scale μ can now be written as,

$$\alpha_a^{-1}(\mu) = \alpha_a^{-1}(M_Z) - \frac{b_0^a}{2\pi}\log\frac{\mu}{M_Z} - \sum_{i\ \text{with}\ m_i<\mu}\frac{d_i^a}{2\pi}\log\frac{\mu}{m_i}. \tag{4}$$

If we now choose

$$d_i^a - d_i^b = k_i(b_0^a - b_0^b), \tag{5}$$

then it is clear that Eq. (2) will remain intact. Hence, we can achieve gauge coupling unification even with the presence of intermediate mass scales, and this is independent of the values of m_i. But unlike complete multiplets of, say, SU(5), the unification scale changes in this case [25]. Let us assume that the gauge coupling constants now unify at a scale $M_{\rm GUT}$. We can now rewrite Eq. (3) as

$$\alpha_a^{-1}(M_Z) - \alpha_b^{-1}(M_Z) = -\frac{b_0^a - b_0^b}{2\pi}\log\frac{M_Z}{M_{\rm GUT}} - \sum_{i=1,\cdots,N}\frac{d_i^a - d_i^b}{2\pi}\log\frac{m_i}{M_{\rm GUT}}. \quad (6)$$

Comparing Eqs. (3) and (6), we can now write the new unification scale $M_{\rm GUT}$ in terms of the unification scale M_0 in the MSSM,

$$M_{\rm GUT} = M_0 \prod_{i=1,2,\cdots,N}\left(\frac{m_i}{M_0}\right)^{\kappa_i}, \quad \text{where } \kappa_i = k_i \Big/ \left(1 + \sum_{j=1,2,\cdots,N} k_j\right). \quad (7)$$

The change in the unified value of the gauge couplings, $\delta\alpha^{-1}(M_{\rm GUT})$, can also be written down explicitly,

$$\delta\alpha^{-1}(M_{\rm GUT}) = \frac{1}{2\pi}\sum_{i=1,2,\cdots,N}\left(d_i^a - \kappa_i b_0^a - \kappa_i \sum_{j=1,2,\cdots,N} d_j^a\right) \times \log\frac{m_i}{M_0}. \quad (8)$$

An example of magic fields is the combination of fields ϕ_Q, $\phi_{\bar{Q}}$ and ϕ_G whose transformation properties under the SM gauge group are given by $(3, 2)_{\frac{1}{6}}$, $(\bar{3}, 2)_{-\frac{1}{6}}$, and $(8, 1)_0$, respectively. Here the first number in the bracket is the SU(3) representation and the second number refers to the SU(2) representation. The number outside the bracket is the hypercharge of the multiplet. Note that the individual fields above are not magic fields, but the combination as a whole satisfies the magic field condition of Eq. (5). The set of fields mentioned above can be obtained from the SO(10) complete multiplets 16, $\bar{16}$, and 45 after spontaneous symmetry breaking [23].

III. MASS SPECTRUM OF THE MAGIC MESSENGER MODELS

In this section, we will derive some general properties of the magic messenger models, where unlike models of ordinary gauge mediation, the superpotential also contains bare mass terms allowed by symmetry. But before we go to the details of our model, let us first discuss those models of GMSB where nonuniversal gaugino masses have been obtained and their qualitative differences from our model.

In ordinary gauge mediation models, the messenger fields are complete multiples of SU(5), like $5 \oplus \bar{5}$. Addition of such complete multiplets changes the beta functions equally for all the SM gauge groups at any scale. Clearly, this does not change the universality of the gaugino masses. Even if all possible renormalizable terms are considered in the superpotential, the situation does not change and universality is maintained. But instead of SU(5) multiplets, if one uses SU(2) and SU(3) irreducible representations and writes the most general superpotential (like models of EOGM with doublet-triplet splitting [24]), then nonuniversal gaugino masses can be achieved only if these doublets and triplets are charged differently under some global symmetry. But to achieve gauge coupling unification at the same time, the masses of the messenger fields should satisfy some constraints. In generalized messenger models, one can easily obtain nonuniversal gaugino masses, but this type of model generally bypasses the question of unification by arguing that there may be some other fields (not messengers of SUSY breaking) in the theory that are charged under the SM, and using these fields it is always possible to get successful unification. If one does not assume this then messenger masses get constrained again. Another generalized messenger model is also available in the literature [26], where messenger masses are not constrained but the grand unified theory (GUT) used there is an anomalous U(1) GUT.

The models we are proposing are also generalized messenger models, but here the messenger fields are magic fields. This class of models has two main differences with other generalized messenger models: (a) gauge coupling unification is independent of messenger scales, and (b) changes in beta functions for each added messenger satisfy the magic relation of Eq. (5). The second property has nontrivial consequences, as we will see in the next two sections.

A. The models

Our models consists of (1) N pairs of magic messenger fields, each pair consisting of $(\phi, \tilde{\phi})$ where ϕ ($\tilde{\phi}$) transforms under some representation (its conjugate representation) of the SM gauge group, and (2) a spurion field X which is a Standard Model gauge singlet but can have charges under some other symmetries like the R symmetry. Note that these ϕ fields are in general not single irreducible representations; they can be a set of fields (each transforming under an irreducible representation) that satisfy the magic condition of Eq. (5). We assume that the field X gets a vacuum expectation value (VEV) through some dynamics of the hidden sector, $\langle X\rangle = M + \theta^2 F$. For the sake of calculational simplicity, we make the assumption that two different pairs of magic messengers either transform under the same representation of the gauge group or have no constituent fields having the same transformation property. This allows us to subdivide the messenger field pairs into different sets (labeled by p), where all members of a set have the same representation. Note that a set may consist of either one pair of messenger fields or many pairs of them. We label the different members (a particular pair of magic messengers) of a set p by the index i_p. For example, if a particular set p has five pairs of magic

messengers, then i_p runs from 1 to 5. We now write the renormalizable superpotential as

$$W = \sum_p \sum_{i_p, j_p} \left(\lambda^p_{i_p j_p} X + m^p_{i_p j_p} \right) \tilde{\phi}_{i_p} \phi_{j_p}, \tag{9}$$

where the form of the matrices λ^p and m^p are determined by global (R and/or non-R) symmetries of the theory. Note that, in general, different constituent fields of any magic field can get different masses and couplings. But to form a magic field, these constituent fields need to share the same mass. We treat the magic fields (ϕ_{i_p}'s) as if they are irreducible representations of some group and write the couplings in the superpotential because this assumption automatically ensures the above requirement (of equality of the masses of the constituent fields of each the magic messenger fields). The above superpotential is symmetric under the interchange of ϕ_{i_p} field with $\tilde{\phi}_{i_p}$ and vice versa. This symmetry is called the messenger parity, and it helps us to get rid of the dangerous Fayet-Iliopoulos terms.[1] Throughout this paper we will call this class of models "magic messengers in gauge mediation" (MMGM).

To calculate the soft terms, we need to write the Lagrangian in mass eigenstates of fermion fields and scalar fields. Using biunitary transformations on the superfields, we first make fermion mass matrices of each set diagonal and real: $M^p_f = \text{diag}(\cdots, m_{i_p}, \cdots)$. In this basis the Kähler term will not change. The matrices $\lambda^p F$ will change, but for brevity we keep the same symbols. Messenger parity and CP conservation imply that these matrices should be real and symmetric. Going to the basis $\phi_{\pm p} = \frac{1}{\sqrt{2}}(\cdots, \phi_{i_p} \pm \tilde{\phi}^*_{i_p}, \cdots)^T$, we can bring the sfermion mass squared matrix of any set in the block-diagonal form with two blocks, $M^2_{\pm p} = (M^p_f)^2 \pm \lambda^p F$. Now these two matrices can be diagonalized as $U^{p\dagger}_{\pm} M^2_{\pm p} U^p_{\pm}$ with eigenvalues $m^2_{\pm i_p}$. We define the following combinations of U matrices which will be used in the next section,

$$\begin{aligned} \mathcal{A}^{p\pm}_{i_p j_p} &= U^{p\dagger}_{\pm i_p j_p} U^p_{\pm j_p i_p} \quad \text{and} \\ \mathcal{B}_{i_p j_p} &= \sum_{k_p l_p} (U^{p\dagger}_{+ i_p k_p} U_{-k_p j_p})(U^{p\dagger}_{- j_p l_p} U_{+ l_p i_p}). \end{aligned} \tag{10}$$

B. Gaugino masses

The expression for gaugino masses at the messenger scale can be written as,

$$M_a = \frac{\alpha_a}{4\pi} \sum_p d^a_p \Lambda^G_p \tag{11}$$

where d^a_p is the Dynkin index of the magic messenger pairs in the set labeled by p corresponding to the gauge group label a, the superscript G in Λ refers to the gaugino sector, and Λ^G_p is given by [22]

$$\Lambda^G_p = 2 \sum_{i_p, j_p \pm} (\pm) \mathcal{A}^{p\pm}_{j_p i_p} \frac{m_{i_p} m^2_{\pm j_p}}{m^2_{\pm j_p} - m^2_{i_p}} \log\left(\frac{m_{\pm j_p}}{m_{i_p}} \right)^2. \tag{12}$$

Here Λ^G_p are independent of the SM gauge group. However, the presence of d^a_p in the expression for gaugino masses implies that the ratio of gaugino masses is not equal to the ratio of α_a's. This means that the gaugino masses are nonuniversal in this class of models. Apparently, it seems that the gaugino masses are completely independent, but actually this is not true. Their ratio satisfies some beautiful structure. The ratio of the gaugino masses can be written as

$$\begin{aligned} &M_1 : M_2 : M_3 \\ &= 1 : \frac{\alpha_2}{\alpha_1}\left[1 + (b^{(2)}_0 - b^{(1)}_0)\zeta\right] : \frac{\alpha_3}{\alpha_1}\left[1 + (b^{(3)}_0 - b^{(1)}_0)\zeta\right], \end{aligned} \tag{13}$$

where

$$\zeta = \frac{\sum_p k_p \Lambda^G_p}{\sum_p d^{(1)}_p \Lambda^G_p}. \tag{14}$$

The value of ζ can be zero, positive or negative. All the gaugino mass parameters become equal if

$$\begin{aligned} \zeta = \zeta_0 &= -\frac{\alpha_3 - \alpha_2}{\alpha_3(b^{(3)}_0 - b^{(1)}_0) - \alpha_2(b^{(2)}_0 - b^{(1)}_0)} \\ &= -\frac{\alpha_2 - \alpha_1}{\alpha_2(b^{(2)}_0 - b^{(1)}_0)}, \end{aligned}$$

where in the last step we use Eq. (2). Any arbitrary ζ can always be written as

$$\zeta = \zeta_0 + \tilde{\zeta}. \tag{15}$$

In that case Eq. (13) takes the form,

$$\begin{aligned} M_1 : M_2 : M_3 &= 1 : 1 + \frac{\alpha_2}{\alpha_1}\left(b^{(2)}_0 - b^{(1)}_0\right)\tilde{\zeta} : 1 + \frac{\alpha_3}{\alpha_1}\left(b^{(3)}_0 - b^{(1)}_0\right)\tilde{\zeta}, \\ &= 1 : 1 - \frac{28}{5}\frac{\alpha_2}{\alpha_1}\tilde{\zeta} : 1 - \frac{48}{5}\frac{\alpha_3}{\alpha_1}\tilde{\zeta}. \end{aligned} \tag{16}$$

It is now clear from Eq. (16) that various ratios among the gaugino masses can be obtained, (a) for negative $\tilde{\zeta}$, one gets normal hierarchy, (b) for $\tilde{\zeta} = 0$, all the gaugino masses are equal, and, (c) for nonzero positive $\zeta \leq \frac{5\alpha_1}{48\alpha_3}$, one gets inverted hierarchy. For $\zeta > \frac{5\alpha_1}{48\alpha_3}$, some more patterns can be achieved.

So to conclude this section, the gaugino sector of this class of models can be parametrized by two free parameters: one of them can be taken as the mass of the U(1) gaugino and the other one is the ζ (or $\tilde{\zeta}$) parameter. These two parameters can be tuned to get phenomenologically interesting ratios among the gaugino masses.

[1] This Fayet-Iliopoulos term is proportional to the VEV of the scalar component of the U(1) current superfield J. Under messenger parity $J \to -J$, because the fields $\tilde{\phi}_{i_p}$ transform under the conjugate representation of the fields ϕ_{i_p}. Hence, due to messenger parity, VEV of J vanishes [13,16].

TABLE I. The values of a, b, c, and d parameters for six benchmark points and the corresponding numerical values for the quantities M_1, $\tilde{\zeta}$, A_1, and η. The values of m_1, m_2, and m_3 are 1.0×10^{14} GeV. The parameters a, b, c, and d are given in units of 10^{18} GeV^2.

Benchmark points	a	b	c	d	M_1 (GeV)	$\tilde{\zeta}$	A_1 (10^8 GeV^2)	η (10^{-5})
1	0.85	80	0.85	0.60	97.304	−0.1914	2.0534	−1.4061
2	0.80	70	0.80	0.90	95.165	−0.2794	1.5722	−4.1320
3	0.80	70	0.80	1.2	98.373	−0.3527	1.5722	−7.3458
4	0.80	70	0.80	1.4	100.51	−0.3989	1.5722	−9.9983
5	0.80	70	0.80	1.6	102.65	−0.4432	1.5723	−13.059
6	0.80	70	0.80	1.8	104.79	−0.4858	1.5723	−16.527

C. Sfermion masses

The sfermion masses are obtained at the two-loop level in GMSB. In GGM, these are parametrized by three parameters A_a ($a = 1, 2, 3$) for three gauge groups U(1), SU(2), and SU(3). In terms of these three parameters, the expression for the sfermion masses [13] can be written as follows,

$$m_{\tilde{f}}^2 = \sum_a g^4 c_2(f, a) A_a, \tag{17}$$

where $c_2(f, a)$ is the quadratic Casimir of the representation f of the gauge group a. In our class of models, the expression for A_a turns out to be

$$A_a = 2\frac{1}{(16\pi^2)^2}\sum_p d_p^a \Lambda_p^S, \tag{18}$$

where Λ_p^S is given by [22]

$$\Lambda_p^S = 2\sum_{i_p j_p \pm} m_{\pm i_p}^2 \left[\mathcal{A}_{i_p j_p}^{p\pm} \log\left(\frac{m_{\pm i_p}^2}{m_{j_p}^2}\right) - 2\mathcal{A}_{i_p j_p}^{p\pm} \mathrm{Li}_2\left(1 - \frac{m_{j_p}^2}{m_{\pm i_p}^2}\right) + \frac{1}{2}\mathcal{B}_{i_p j_p} \mathrm{Li}_2\left(1 - \frac{m_{\mp j_p}^2}{m_{\pm i_p}^2}\right)\right]. \tag{19}$$

The quantities Λ_p^S and A_a are required to be strictly positive in order to have positive sfermion masses.

Ratio of the A_a parameters can be written as,

$$A_1 : A_2 : A_3 = 1 : 1 - \frac{28}{5}\eta : 1 - \frac{48}{5}\eta, \tag{20}$$

where

$$\eta = \frac{\sum_p k_p \Lambda_p^S}{\sum_p d_p^{(1)} \Lambda_p^S}. \tag{21}$$

Note that η cannot be greater than $\eta_0 = \frac{5}{48}$. For $\eta \sim \eta_0$, one has $A_1 > A_2 \gg A_3$. In this limit, from Eq. (17) one can see that soft SUSY breaking squark and Higgs masses will be approximately the same (universal) at the messenger scale. This would in turn render the value of m_{H_u} at weak scale insensitive to the universal scalar masses in the ultraviolet. This can be understood as a consequence of a "focus point" in the RG behavior of m_{H_u} [27,28]. In this case it is possible to have a small μ (supersymmetric mass term for the Higgs) [29,30] and thus a Higgsino-like NLSP. This can lead to very distinct phenomenology [31,32].

IV. AN EXPLICIT MODEL OF MMGM

In this section we construct an explicit model of MMGM. We take two sets of messengers, the first set consists of two pairs of SU(5) $5 + \bar{5}$ fields: ϕ_i, $\tilde{\phi}_i$ with $i = 1, 2$, and the second set contains a magic field: $\phi_3 = \phi_Q + \phi_{\bar{Q}} + \phi_G$. Note that one can write down the required terms for gauge mediation [as given in Eq. (9)], using only ϕ_3 and without invoking its conjugate field $\tilde{\phi}_3$. Moreover, absence of the field $\tilde{\phi}_3$ does not break the messenger parity because the superpotential remains invariant under the interchange of ϕ_Q by $\phi_{\bar{Q}}$ and vice versa. This is why we do not include the $\tilde{\phi}_3$ field in the second set just to make it more economical. In the second set, we will denote the fermion mass by m_3 and the eigenvalues of the scalar mass squared matrix by $m_3^2 \pm d$. For the first set, in the diagonal basis of the fermion mass matrix $M_f = \mathrm{diag}(m_1, m_2)$, the mass squared matrix of the scalars will look like

$$M_{\pm}^2 = \begin{pmatrix} m_1^2 & 0 \\ 0 & m_2^2 \end{pmatrix} \pm \begin{pmatrix} a & b \\ b & c \end{pmatrix}. \tag{22}$$

Clearly, the eigenvalues and the diagonalizing matrices of $M_{\pm}^2$ will involve the quantities a, b, c and, hence, the four parameters M_1, $\tilde{\zeta}$, A_1, and η will also depend on them. Just to give a few examples, in Table I we choose six benchmark points[2] and show the values of a, b, c, d and the corresponding numerical values for M_1, $\tilde{\zeta}$, A_1, and η.

It is well known that among the various models of GMSB, the mass ratio between the sfermions and gauginos is the lowest in the case of ordinary gauge mediation models [20] [which can be obtained by setting $b = 0$ in Eq. (22)]. In order to increase this ratio, b should be made large compared to a and c. The parameter d is related to the magic part of the model. So changing d, one can increase

[2]In our models, gravitino mass is in the range of 17 to 20 GeV. If we assume gravitino to be the LSP, then big bang nucleosynthesis will be problematic because of large neutralino lifetime. This problem can be easily solved in the axino dark matter models, where the lifetime of the lightest neutralino can be less than. 1 sec [33–35].

TABLE II. Masses of the lightest neutralino, next-to-lightest neutralino, lightest chargino, and lightest CP even neutral Higgs for the six benchmark points. All other SUSY particles have masses in the multi-TeV range (~ 7 to 15 TeV). Definition of fine-tuning parameters are $\frac{\delta M_Z^2}{M_Z^2}(\mu) = \frac{2\mu^2}{M_Z^2}\left[1 + t_\beta \frac{4\tan^2\beta(\bar{m}_1^2 - \bar{m}_2^2)}{(\bar{m}_1^2 - \bar{m}_2^2)t_\beta - M_Z^2}\right]\frac{\delta\mu^2}{\mu^2}$ and $\frac{\delta M_Z^2}{M_Z^2}(B\mu) = 4t_\beta \tan^2\beta \frac{\bar{m}_1^2 - \bar{m}_2^2}{M_Z^2(\tan^2\beta - 1)^2}$, where $t_\beta = (\tan^2\beta + 1)/(\tan^2\beta - 1)$. Hence, fine-tuning is large.

Benchmark points	$\tan\beta$	$m_{\tilde{\chi}_1^\pm}$ (GeV)	$m_{\tilde{\chi}_2^0}$ (GeV)	$m_{\tilde{\chi}_1^0}$ (GeV)	m_h (GeV)	$m_{\tilde{g}}$ (GeV)	μ (GeV)	BR($\chi_2^0 \to \chi_1^0 h$)	$\frac{\delta M_Z^2}{M_Z^2}(B\mu)$	$\frac{\delta M_Z^2}{M_Z^2}(\mu)$ (10^4)
1	20	203.0	203.0	50.9	124.8	1019	7935	98.908	66.25	1.53
2	25	248.1	248.1	49.0	124.6	1239	7003	96.883	30.83	1.19
3	30	299.4	299.4	50.2	124.8	1482	7024	95.221	19.74	1.19
4	20	332.3	332.3	50.6	124.8	1641	7055	96.076	52.64	1.21
5	20	366.1	366.1	51.3	124.9	1797	7070	95.621	52.92	1.21
6	20	399.7	399.7	51.9	124.9	1950	7085	96.343	53.19	1.22

or decrease the splitting among the gaugino masses. Note that we got $\tilde{\zeta} \sim 10^{-1}$, whereas $\eta \sim 10^{-5}$. So gaugino masses are highly hierarchical (see Table II) but A_a parameters are not. To understand this, one should note that the SU(5) part of this model is not an OGM model but an EOGM model, and b is a hundred times larger than a, c, and d. From Eq. (B.6) and (B.8) of [20], one can see that the off-diagonal element b has no effect on the expression for gaugino masses, whereas it has dominant contribution on the sfermion masses. Using the fact that $\frac{F}{M^2} \sim 10^{-8}$, the expression for the η parameter can be approximated as $\eta \sim -\frac{1}{4}\frac{d^2}{b^2}$. This explains why η is small in this model.

A. Phenomenology: boosted Higgs signal

There are many models of supersymmetry breaking where the soft supersymmetry breaking gaugino mass terms M_1, M_2, and M_3 meet to a common value $m_{1/2}$ at the GUT scale. Now the one-loop renormalization group equations for the three gaugino mass parameters in the MSSM are determined by the same quantities b_a^0 ($a = 1$, 2, 3) which also control the RG running of the three gauge couplings. It then immediately follows that each of the three ratios $\frac{M_a}{g_a^2}$ is one-loop RG invariant. In models of gaugino mass unification (for example, models with minimal supergravity or gauge-mediated boundary conditions), this leads to an interesting relation, M_1:M_2:$M_3 = 1$:2:7 approximately at the TeV scale (modulo two-loop corrections and unknown threshold corrections). Now, if the supersymmetric Higgsino mass parameter $\mu \gg M_1$, M_2, then the physical mass eigenstates consist of a "binolike" lightest neutralino $\tilde{\chi}_1^0$ and a "winolike" next-to-lighest neutralino $\tilde{\chi}_2^0$ and lightest chargino $\tilde{\chi}_1^\pm$. In this case, one has a very good approximation $m_{\tilde{g}} \sim M_3$, $m_{\tilde{\chi}_2^0}, m_{\tilde{\chi}_1^\pm} \sim M_2$, and $m_{\tilde{\chi}_1^0} \sim M_1$. With the increase of the lower bound on squark and gluino masses by the LHC data, their production cross section has been pushed to quite low values ($\sim$ a few fb). On the other hand, the electroweak gaiginos can be sufficiently lighter ($\tilde{\chi}_1^\pm$, $\tilde{\chi}_2^0 \sim 250$ is still allowed even if universality is assumed). Hence, the pair production cross section of the light electroweak gauginos dominates the SUSY production cross section.

In our model, as we have already seen, in general the gaugino mass parameters can be arranged to have any ratio among themselves. In particular, we consider the case where M_1, M_2, and M_3 are much more hierarchical than the ratio 1:2:7. In this case $\tilde{\chi}_1^\pm$ and $\tilde{\chi}_2^0$ lighter than 250 GeV are still allowed. In this section we consider the production of $\tilde{\chi}_1^\pm$, $\tilde{\chi}_2^0\sim$ and their subsequent decays, $\tilde{\chi}_1^\pm \to \tilde{\chi}_1^0 W$ and $\tilde{\chi}_2^0 \to \tilde{\chi}_1^0 h$. The prospect of this channel at 8 TeV LHC in the case of the mSUGRA model has been studied in detail in [36]. It was concluded that an integrated luminosity of 100 fb^{-1} will be needed for a good signal-to-background ratio. Note that unlike mSUGRA in our model, the lightest neutralino χ_1^0 can be considerably lighter than χ_2^0 and, hence, the lightest Higgs boson from the decay of χ_2^0 can be quite boosted.

In Table II we show a few benchmark points that will be used for a detailed signal anlysis. We choose the parameters in our model so as to get different ratios of gaugino masses along with the lightest Higgs boson mass consistent with the recent hints of Higgs signal by the CMS [37] and ATLAS [38] Collaborations. Note that in our case, the branching ratio for the decay $\tilde{\chi}_2^0 \to \tilde{\chi}_1^0 h$ is very large ($> 95\%$). For related discussions on the parameter dependence on this branching ratio and interplay with other decay modes, see Ref. [39].

To generate the mass spectrum of the SUSY particles, we have used the package SUSPECT [40]. SUSYHIT [41] has been used to calculate the corresponding branching ratios. Note that the gluinos are quite heavy for all the benchmark points, and consequently their production cross section is extremely small. For example, for the benchmark point 1, the gluino pair production cross section is about 4 fb (LO) for 8 TeV center-of-mass energy, and it is even smaller for the other benchmark points.

In Fig. 1 we show the transverse momentum distribution of the Higgs in the decay $\tilde{\chi}_2^0 \to \tilde{\chi}_1^0 h$, following the direct

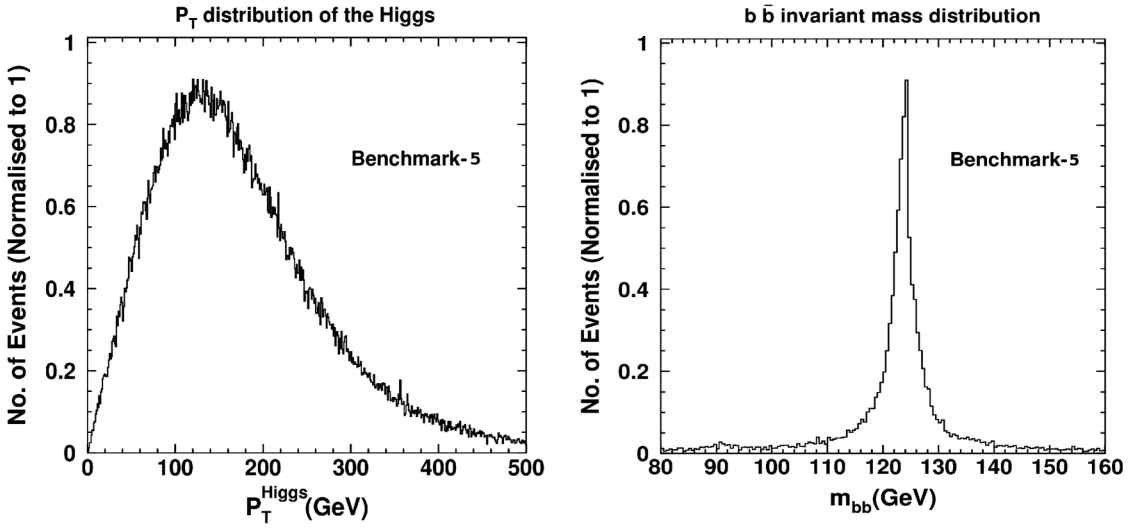

FIG. 1. Left panel: The transverse momentum distribution of the Higgs boson from the decay $\chi_2^0 \to \chi_1^0 h$ following the direct production of $(\chi_1^\pm, \chi_2^0)$ at 8 TeV LHC for our SUSY benchmark point 5. The y axis has been normalized to 1. Right panel: The invariant mass distribution of the reconstructed Higgs boson using the jet substructure algorithm, as described in the text, for our SUSY benchmark point 5. The y axis has been normalized to 1. The figures have been generated using the CERN package PAW [60].

production of $\tilde{\chi}_1^\pm$, $\tilde{\chi}_2^0$ at the LHC with 8 TeV center-of-mass energy. It can be observed that a large fraction of the Higgs bosons has transverse momentum greater than 100 GeV. This allows us to use the jet substructure technique to look for Higgs in the decays of directly produced electroweak gauginos.

The use of jet substructure for the reconstruction of hadronic decays of boosted W, Z, Higgs bosons and top quarks has received considerable attention in recent years [42–44]. A study of jet substructure in the context of a search for a heavy Higgs boson decaying to WW was first carried out in Ref. [45]. More recently, Butterworth, Davison, Rubin, and Salam (BDRS) [46] studied the case of a light Higgs boson ($m_H \sim 120$ GeV) produced in association with an electroweak gauge boson. The leptonic decay of the associated vector boson provides an efficient trigger for these events. The BDRS algorithm involves a technique using the mass-drop and the filtering to transform the high-p_T WH, $ZH(H \to b\bar{b})$ channel into one of the best channels for discovery of Standard Model Higgs with small mass at the LHC.

In this section we adopt the BDRS method for tagging hadronically decaying Higgs boson. We describe below the exact procedure adopted in our analysis in order to implement this along with our other selection cuts.

We first cluster all the stable final state particles (excluding leptons, neutrinos, and neutralinos) into "fat jets," using the Cambridge-Aachen (CA) algorithm [47,48], as implemented by the FASTJET package [49] with R parameter of 1.2. We then select the jets with transverse momentum $p_T > 100$ GeV and pseudorapidity $|\eta| < 2.5$. We now perform the jet substructure analysis on the hardest jet following the BDRS prescription. Here, we closely follow the discussion of Ref. [46], mentioning our specific choices of parameters as the occasion arises. The first step is to select a jet-j and apply the following procedure:

(1) Undo the last clustering step of the jet-j to get two subjets. Label the two subjets j_1 and j_2 so that $m_{j_1} > m_{j_2}$. (Remember that at each step during the CA clustering, the masses of the protojets to be combined are recorded).

(2) Define $\mu = \frac{m_{j_1}}{m_j}$, $y_{\rm cut} = \frac{\min(p_{Tj_1}^2, p_{Tj_2}^2)}{m_j^2} \Delta R_{j_1,j_2}^2$. Here $\Delta R_{j_1,j_2}$ is the separation between the two subjets j_1 and j_2 in the pseudorapidity(η)- azimuthal angle (ϕ) plane. If $\mu < \mu_{\rm cut}$ (significant mass drop) and $y > y_{\rm cut}$ (the splitting of the hard jet-j into two subjets j_1 and j_2 is not too asymmetric), then go to step 4. We use $\mu_{\rm cut} = 0.4$ and $y_{\rm cut} = 0.1$ in our analysis.

(3) Otherwise, redefine $j = j_1$ and go back to step 1.

(4) Take the constituents of the mother jet-j and recluster them with the Cambridge-Aachen algorithm with an R parameter of $R_{\rm filt} = \min(\frac{\Delta R_{j_1,j_2}}{2}, 0.4)$. Construct n new subjets $j_1^{\rm filt}, j_2^{\rm filt}, j_3^{\rm filt}, \ldots j_n^{\rm filt}$, ordered in descending p_T. This step is supposed to reduce the degradation of resolution on jets caused by underlying events.

(5) Require the two hardest of the subjets $j_1^{\rm filt} \ldots j_n^{\rm filt}$ to have b tags.

(6) Define $j^{\rm higgs} = \sum_{i=1}^{\min(n,3)} j_i^{\rm filt}$. This step captures the dominant $\mathcal{O}(\alpha_s)$ radiation from the Higgs decay, while eliminating much of the contamination from underlying events [46].

The parameters involved in this method can be, in principle, optimized event by event [50]. In our analysis, these parameters have been set to fixed values as already mentioned above. In Fig. 1 we show the distribution of the reconstructed Higgs mass using the above BDRS

TABLE III. Event summary for the signal and the backgrounds after individual cuts as described in the text for LHC8. In the second column, the leading order (LO) cross sections have been obtained using PYTHIA and ALPGEN. While calculating the final cross section after Cut V, the NLO cross sections for signal (from PROSPINO) and appropriate K factors (whenever available) for the backgrounds, as mentioned in the text, have been used. The b-tagging efficiency has also been multiplied. K and L in the third column stand for 10^3 and 10^5, respectively. Note that the number of simulated events is always more than the expected number of events at the LHC (at 30 fb^{-1}) for both the signal and backgrounds.

			Number of events after individual cuts						
Process	Cross section (LO)	Simulated events	Cut I	Cut II	Cut III	Cut IV	Cut V	Cross section after Cut V	$\frac{S}{\sqrt{B}}$(30 fb^{-1})
			Signal						
Benchmark 1	533 fb	50 K	681	178	71	47	28	0.21 fb	≈ 4
Benchmark 2	241 fb	50 K	1220	311	150	106	84	0.27 fb	≈ 5.1
Benchmark 3	108 fb	50 K	1729	475	287	201	177	0.27 fb	≈ 5.1
Benchmark 4	71 fb	50 K	2112	552	356	270	246	0.23 fb	≈ 4.4
Benchmark 5	45 fb	50 K	2697	788	522	380	341	0.21 fb	≈ 4
Benchmark 6	30 fb	50 K	3092	904	655	488	449	0.21 fb	≈ 4
			Background						
$t\bar{t}$(0–100)	48.3 pb	40 L	1126	274	29	3	0		
$t\bar{t}$(100–200)	36.6 pb	30 L	976	234	26	6	1	0.0119 fb	
$t\bar{t}$(200–300)	7.8 pb	5 L	157	40	6	3	2	0.0306 fb	
$t\bar{t}$(300–500)	1.8 pb	1.5 L	24	5	1	0	0		
$t\bar{t}$(500–∞)	134 fb	10 K	0	0	0	0	0		
$W(\rightarrow l\nu_l)b\bar{b}$ $l = e, \mu, \tau$	3 pb	201308	64	35	3	2	0		
Wh	549 fb	50 K	401	125	9	5	2	0.0108	
WZ	13 pb	8 L	11	3	0	0	0		
Zh	296 fb	20 K	167	4	0	0	0		
$Z(\rightarrow l^+l^-)b\bar{b}$ $l = e, \mu, \tau$	2 pb	126581	26	5	0	0	0		
$t(\rightarrow e\nu_e b)b$	308 fb	36817	6	5	0	0	0		
tbW	18.7 pb	597812	156	43	4	2	2	0.0306 fb	
Total Background								0.084 fb	

prescription for our SUSY benchmark point 5. For the other benchmark points, the distributions are qualitatively the same, and we do not show them here.

We also impose a b-jet reconstruction efficiency of 70% [51] in our analysis. We then require the following preselection cuts [36,52,53]:

(i) Cut I: We require the mass of j^{higgs} to be in the window [119, 129].

(ii) Cut II: Exactly one isolated lepton (ℓ) with $p_T(\ell) >$ 20 GeV and no isolated lepton with 10 GeV$< p_T(\ell) <$ 20 GeV.

(iii) Cut III: The transverse mass of the lepton (ℓ)-missing P_T system $M_T^{(\ell \not{p}_T)} > 90$ GeV.

(iv) Cut IV: At this stage we again construct "normal," jets using the CA algorithm with R parameter of 0.5, $|\eta| < 2.5$, $P_T > 50$ GeV. We then calculate H_T, which is defined as the scalar sum of the P_T's of all these "normal" jets. We define $R_T^{b\bar{b}} = \frac{p_{Tb_1} + p_{Tb_2}}{H_T}$. Remember that p_{Tb_1} and p_{Tb_2} are the transverse momenta of the two subjets j_1^{filt} and j_2^{filt} which are by now identified as two b-jets. We demand $R_T^{b\bar{b}} > 0.9$.

(v) Cut V: Events are selected with $\not{p}_T > 125$ GeV.

In Table III and IV, we show the signal and backgrounds after each selection cut for 8 and 14 TeV center-of-mass energies, respectively. For all the signal points, we use the next-to-leading order (NLO) cross section from PROSPINO [54]. We simulate the $t\bar{t}$, Wh, WZ, and Zh backgrounds using PYTHIA [55]. For the Wbb, Zbb, and single top backgrounds, we generate the unweighted event files in ALPGEN [56] and then use the ALPGEN-PYTHIA interface (including matching of the matrix element hard partons and shower generated jets, following the Mangano's prescription [57]) to perform the showering and implement our event selection cuts. For the $t\bar{t}$ background, a K factor of 2 has been used. We use the CTEQ6L parton distribution functions and set top mass at 172.9 GeV in our analysis. We have also used the new LHC PYTHIA 6.4 TUNE Z2* for the correct description of the underlying events [58]. We see that $S/\sqrt{B}$ of about 4–6 can be obtained at 8 TeV LHC with an integrated luminosity of about 30 fb^{-1}. At the 14 TeV LHC the situation is much better, and even with 15 fb^{-1} we get a fairly good number of events, while the backgrounds are totally under control with our selection cuts. In Table III (Table IV), we have simulated at least 30 fb^{-1} (15 fb^{-1}) of events for both the signal points as well as the

TABLE IV. Event summary for the signal and the backgrounds after individual cuts as described in the text for LHC14. In the second column, the LO cross sections have been obtained using PYTHIA and ALPGEN. While calculating the final cross section after Cut V, the NLO cross sections for signal (from PROSPINO) and appropriate K factors (whenever available) for the backgrounds, as mentioned in the text, have been used. The b-tagging efficiency has also been multiplied. K and L in the third column stand for 10^3 and 10^5, respectively. Note that the number of simulated events is always more than the expected number of events at LHC (at 15 fb^{-1}) for both the signal and backgrounds.

Process	Cross section (LO)	Simulated events	Number of events after individual cuts					Cross section after Cut V
			Cut I	Cut II	Cut III	Cut IV	Cut V	
			Signal					
Benchmark 1	1.4 pb	50 K	769	186	78	54	29	0.53 fb
Benchmark 2	681 fb	50 K	1282	327	156	119	92	0.73 fb
Benchmark 3	332 fb	50 K	1857	465	288	198	169	0.73 fb
Benchmark 4	226 fb	50 K	2363	626	392	274	238	0.73 fb
Benchmark 5	155 fb	50 K	2792	746	499	359	321	0.67 fb
Benchmark 6	105 fb	50 K	3125	843	592	416	373	0.53 fb
			Background					
$t\bar{t}(50-\infty)$	335 pb	100 L	3467	913	128	11	3	0.098 fb
$W(\rightarrow l\nu_l)b\bar{b}$ $l = e, \mu, \tau$	5.45 pb	429871	148	86	7	6	0	
Wh	1.24 pb	50 K	446	108	7	3	1	0.012 fb
WZ	29 pb	8 L	20	5	0	0		
Zh	674 fb	50 K	449	6	0	0	0	
$Z(\rightarrow \ell^+\ell^-)b\bar{b}$ $\ell = e, \mu, \tau$	7.4 pb	607607	116	23	5	4	0	
tb	5.6 pb	182974	16	3	0	0	0	
$t(\rightarrow \ell\nu_\ell b)bW(\rightarrow \text{had})$ $\ell = e, \mu, \tau$	17.1 pb	499383	125	65	11	0	0	
$t(\rightarrow \text{had})bW(\rightarrow \ell\nu_\ell)$ $\ell = e, \mu, \tau$	17.1 pb	665454	229	127	14	3	0	
Total Background								0.11 fb

backgrounds. Note that the detector and other experimental effects will degrade the signal significance somewhat. We have checked that the numbers change by $\sim$10% if a Gaussian smearing is added to the transverse momenta of the jets and the missing transverse momentum, though a faithful quantification of the detector effects is beyond the scope of this work.

As the masses of $\tilde{\chi}_1^\pm$ and $\tilde{\chi}_2^0$ increase (see Table II), their production cross section gradually decreases. This tends to reduce the signal-to-background ratio. On the other hand, from benchmark 1 to benchmark 6, the mass difference between $\tilde{\chi}_2^0$ and $\tilde{\chi}_1^0$ also increases. This makes the Higgs boson more boosted, thereby increasing the efficiency of the jet substructure algorithm. With the increasing mass of $\tilde{\chi}_2^0$ in Table II, these two opposite effects keep competing with each other. This is why the signal efficiency initially increases with increasing $\tilde{\chi}_2^0$ mass but again starts falling down because of the rapid decrease in the cross section.

V. CONCLUSION

In this paper we have implemented magic fields as messengers of SUSY breaking in GMSB. One of the advantages of using magic fields as messengers over other generalized messengers is that achievement of unification is independent of the masses of the magic messengers.

In our model the gaugino sector is parametrized by only the following two independent parameters: one of them can be taken to be the U(1) gaugino mass and the second one is the $\tilde{\zeta}$ parameter [Eqs. (14) and (15)]. The ζ parameter can be tuned to get various hierarchies among the gaugino masses which can lead to distinct phenomenological consequences.

The sfermion sector can also be characterized by only two independent quantities. These are the U(1) A parameter A_1 (Eq. (18)) and the parameter η (Eq. (21)). Choosing η, different hierarchies between the squark and slepton masses can be achieved. When the value of η is close to its upper limit η_0, the squark and Higgs masses at the messenger scale tend to be almost the same. This allows one to have small μ parameter and Higgsino-like NLSP, similar to the models of EOGM with large doublet-triple splitting.

We focus on the region of parameter space, where a comparatively larger splitting (about 1:6) between the U(1) and SU(2) gaugino masses is achieved along with the lightest supersymmetric Higgs boson mass of about 125 GeV. We consider the direct electroweak production of $\chi_1^\pm$ and χ_2^0 with $\chi_1^\pm$ decaying to the lightest neutralino χ_1^0 and a W boson, and χ_2^0 decaying to χ_1^0 and the lightest Higgs h. Because of the large splitting between χ_2^0 and χ_1^0,

the produced Higgs boson is expected to have quite large transverse momentum. Motivated by this, we have analyzed the $\ell + b\bar{b} + \not{p}_T$ channel using the jet substructure technique. We have simulated all possible backgrounds for this final state and conclude that while $S/\sqrt{B} \sim 4$–6 is viable (for the mass ranges of charginos and neutralinos we have considered) at 8 TeV LHC with a integrated luminosity of 30 fb^{-1}, LHC14 can do much better, and even with 15 fb^{-1} of data, a decent number of signal events over the backgrounds is expected. In our analysis, we have not considered any detector effect that is expected to degrade the signal significance to some extent.

A detailed exploration of other phenomenological consequences of this class of models, including constraints from flavor physics as well as other low-energy experiments, should be carried out and we plan to perform such a study in a future publication [59].

ACKNOWLEDGMENTS

P. B. would like to thank Professor Palash B. Pal for encouragement and Diego Marques for some comments. P. B. is also grateful to Professor Amol Dighe for his kind hospitality at the Department of Theoretical Physics of TIFR, where a large part of this project was completed. D. G. thanks Professor Monoranjan Guchait and Dr. Dipan Sengupta for insightful discussions and technical help in the event simulation. D. G. would also like to thank Professor Amol Dighe for his continuous support.

[1] Sandra Kortner (ATLAS Collaboration), in *Proceedings of the XLVII Rencontres de Moriond, Electroweak Session* (2012), Report No. ATLAS-CONF-2012-019.
[2] Marco Pieri (CMS Collaboration), arXiv:1205.2907.
[3] Steven Lowette (ATLAS and CMS Collaborations), arXiv:1205.4053
[4] J. Wess and J. Bagger, *Supersymmetry and Supergravity* (Princeton University Press, Princeton, NJ, 1992).
[5] S. P. Martin, in *Perspectives on Supersymmetry II*, edited by G. L. Kane (World Scientific, Singapore, 1998), p. 1.
[6] H. P. Nilles, Phys. Rep. **110**, 1 (1984).
[7] M. Dine, W. Fischler, and M. Srednicki, Nucl. Phys. **B189**, 575 (1981).
[8] S. Dimopoulos and S. Raby, Nucl. Phys. **B192**, 353 (1981).
[9] M. Dine and W. Fischler, Phys. Lett. **110B**, 227 (1982).
[10] M. Dine and W. Fischler, Nucl. Phys. **B204**, 346 (1982).
[11] G. F. Giudice and R. Rattazzi, Phys. Rep. **322**, 419 (1999).
[12] C. R. Nappi and B. A. Ovrut, Phys. Lett. **113B**, 175 (1982).
[13] P. Meade, N. Seiberg, and D. Shih, Prog. Theor. Phys. Suppl. **177**, 143 (2009).
[14] J. Distler and D. Robbins, arXiv:0807.2006.
[15] K. A. Intriligator and M. Sudano, J. High Energy Phys. 11 (2008) 008.
[16] Z. Komargodski and N. Seiberg, J. High Energy Phys. 03 (2009) 072.
[17] L. M. Carpenter, M. Dine, G. Festuccia, and J. D. Mason, Phys. Rev. D **79**, 035002 (2009).
[18] M. Buican, P. Meade, N. Seiberg, and D. Shih, J. High Energy Phys. 03 (2009) 016.
[19] T. Kobayashi, Y. Nakai, and R. Takahashi, J. High Energy Phys. 01 (2010) 003.
[20] T. T. Dumitrescu, Z. Komargodski, N. Seiberg, and D. Shih, J. High Energy Phys. 05 (2010) 096.
[21] S. P. Martin, Phys. Rev. D **55**, 3177 (1997).
[22] D. Marques, J. High Energy Phys. 03 (2009) 038.
[23] L. Calibbi, L. Ferretti, A. Romanino, and R. Ziegler, Phys. Lett. B **672**, 152 (2009).
[24] C. Cheung, A. L. Fitzpatrick, and D. Shih, J. High Energy Phys. 07 (2008) 054.
[25] S. P. Martin and P. Ramond, Phys. Rev. D **51**, 6515 (1995).
[26] H. Kawase, N. Maekawa, and K. Sakurai, J. High Energy Phys. 01 (2010) 027.
[27] J. L. Feng, K. T. Matchev, and T. Moroi, Phys. Rev. Lett. **84**, 2322 (2000).
[28] J. L. Feng, K. T. Matchev, and T. Moroi, Phys. Rev. D **61**, 075005 (2000).
[29] K. Agashe and M. Graesser, Nucl. Phys. **B507**, 3 (1997).
[30] K. Agashe, Phys. Rev. D **61**, 115006 (2000).
[31] J. T. Ruderman and D. Shih, J. High Energy Phys. 08 (2012) 159.
[32] Y. Kats, P. Meade, M. Reece, and D. Shih, J. High Energy Phys. 02 (2012) 115.
[33] T. Asaka and T. Yanagida, Phys. Lett. B **494**, 297 (2000).
[34] L. Covi, J. E. Kim, and L. Roszkowski, Phys. Rev. Lett. **82**, 4180 (1999).
[35] L. Covi, H.-B. Kim, J. E. Kim, and L. Roszkowski, J. High Energy Phys. 05 (2001) 033.
[36] D. Ghosh, M. Guchait, and D. Sengupta, Eur. Phys. J. C **72**, 2141 (2012).
[37] S. Chatrchyan *et al.* (CMS Collaboration), Phys. Lett. B **710**, 26 (2012).
[38] G. Aad *et al.* (ATLAS Collaboration), Phys. Lett. B **710**, 49 (2012).
[39] S. Gori, P. Schwaller, and C. E. M. Wagner, Phys. Rev. D **83**, 115022 (2011).
[40] A. Djouadi, J.-L. Kneur, and G. Moultaka, Comput. Phys. Commun. **176**, 426 (2007).
[41] A. Djouadi, M. M. Muhlleitner, and M. Spira, Acta Phys. Pol. B **38**, 635 (2007).
[42] G. D. Kribs, A. Martin, T. S. Roy, and M. Spannowsky, Phys. Rev. D **82**, 095012 (2010).
[43] A. Abdesselam, E. B. Kuutmann, U. Bitenc, G. Brooijmans, J. Butterworth, P. Bruckman de Renstrom,

D. Buarque Franzosi, R. Buckingham *et al.*, Eur. Phys. J. C **71**, 1661 (2011).
[44] A. Altheimer, S. Arora, L. Asquith, G. Brooijmans, J. Butterworth, M. Campanelli, B. Chapleau, A. E. Cholakian *et al.*, arXiv:1201.0008.
[45] M. H. Seymour, Z. Phys. C **62**, 127 (1994).
[46] J. M. Butterworth, A. R. Davison, M. Rubin, and G. P. Salam, Phys. Rev. Lett. **100**, 242001 (2008).
[47] Y. L. Dokshitzer, G. D. Leder, S. Moretti, and B. R. Webber, J. High Energy Phys. 08 (1997) 001.
[48] M. Wobisch and T. Wengler, arXiv:hep-ph/9907280.
[49] M. Cacciari and G. P. Salam, Phys. Lett. B **641**, 57 (2006).
[50] D. E. Kaplan, K. Rehermann, M. D. Schwartz, and B. Tweedie, Phys. Rev. Lett. **101**, 142001 (2008).
[51] CMS Collaboration, Report No. CMS-PAS-BTV-11-001.
[52] M. Guchait and D. Sengupta, Phys. Rev. D **84**, 055010 (2011).
[53] D. Ghosh, M. Guchait, S. Raychaudhuri, and D. Sengupta, Phys. Rev. D **86**, 055007 (2012).
[54] W. Beenakker, R. Hopker, and M. Spira, arXiv:hep-ph/9611232.
[55] T. Sjostrand, S. Mrenna, and P. Z. Skands, J. High Energy Phys. 05 (2006) 026.
[56] M. L. Mangano, M. Moretti, F. Piccinini, R. Pittau, and A. D. Polosa, J. High Energy Phys. 07 (2003) 001.
[57] J. Alwall, S. Hoche, F. Krauss, N. Lavesson, L. Lonnblad, F. Maltoni, M. L. Mangano, M. Moretti *et al.*, Eur. Phys. J. C **53**, 473 (2008).
[58] A. Knutsson, talk given at CERN, http://indico.cern.ch/getFile.py/access?contribId=13 &sessionId=2 &resId=0 &materialId=slides &confId=140054.
[59] P. Byakti and D. Ghosh (unpublished).
[60] Physics Analysis Workstation (PAW), http://wwwasd.web.cern.ch/wwwasd/paw/.